Experimental study on flow resistance in a vertical 3 × 3 rod bundle channel under natural circulation conditions

ZHU Zhiqiang[1], TIAN Chunping[1], REN Tingting[1], YAN Changqi[1], and WANG Jianjun[1]

1. Fundamental Science on Nuclear Safety and Simulation Technology Laboratory, Harbin Engineering University, Harbin 150001, China (zhuzhiqiang@hrbeu.edu.cn; wangjianjunheu@163.com)

Abstract: In order to study and analyze flow resistance characteristics in a 3 × 3 rod bundle channel, a natural circulation loop was set up and a series of experiments were conducted. For single-phase flow, the flow regime is divided and the transition Reynolds number is considered as 800. The flow transition is recognized by the slope change of friction factor curve since the flow transition in the rod bundle channel is not as obvious as that in round pipe. There is a slight change at Reynolds number 800 for the grid spacer local resistance coefficient. For two-phase flow resistance, the boiling flow phases are identified to obtain stable two-phase flow. The ONB during the experiment is determined by the wall temperature drop. The variation of pressure drop components, including the gravity pressure drop, the frictional pressure drop and the acceleration pressure drop, is given. For high mass quality conditions, the mass flow rate is observed declining with the increasing heat flux when the frictional pressure drop grows fast. Based on the Chisholm correlation, a new correlation is fitted by experimental results. The comparison against experimental results shows the new correlation can well predict the two-phase frictional pressure drops under given flow conditions.

Keywords: rod bundle; natural circulation; flow transition; frictional resistance; flow boiling

1 Introduction

Rod bundle channels are widely used in pressurized water reactors. Flow characteristics in rod bundle channels are significant to reactor operation safety and reliability. Because of the complex geometric structure, flow characteristics in rod bundle channels show differences compared with regular channels such as round pipes and rectangular channels. Although many researchers investigated the flow characteristics, such as the flow transition, the void fraction and the pressure drops in rod bundle channels, the results of natural circulation flow characteristics are scarce in the public literature. Therefore, it is valuable to do research on the flow resistance in a rod bundle channel under natural circulation conditions.

Much effort has been paid on the flow resistance in rod bundle channel in past decades. It is hard to obtain the theoretical solution of the friction factor owing to the complex channel structure. Rehme [1-2] gave the calculation method for different subchannels and proposed geometrical factors in allusion to different rod bundle structures, thus obtaining the friction factor calculation method of the whole channel. It was also pointed out that the turbulent friction factor can be predicted provided with the laminar value. Cheng & Todreas [3] did research on the frictional resistance for different flow regime and took the geometric structure, like the ratio of rod pitch and rod outer diameter Pi/D, as important factors that influence the frictional resistance. The friction factor calculation method was put forward for the rod bundle in triangle and square array. Moreover, the flow regime was divided and the transition Reynolds number was given. Yan [4] conducted experiments on the flow resistance in a 3 × 3 rod bundle channel under static and rolling motion condition and concluded that the cycle-average friction factor is nearly the same as the stable results. Marek [5] performed an investigation with helium in rod bundle channels respectively containing 9 and 16 smooth tubes in square arrays. The correlations for friction factors were considered to be determined by Pi/D, where $Pi/D < 2.0$. For heated conditions, the friction factor results were different from those in adiabatic conditions unless modified by the wall temperature and the bulk temperature. Lee [6] theoretically analyzed the fluid stress near the wall

and developed a computational model to predict the friction factors for bare rod bundles with low *Pi/D* values. Eifler & Nijsing [7] experimentally investigated the Reynolds number and the rod pitch effect in a hexagonal rod bundle channel. They proposed uniform geometrical friction factors for different Reynolds numbers and rod pitches with surface roughness effect covered.

In terms of two-phase flow resistance characteristics, no uniform method for the two-phase pressure drop calculation has been obtained yet. Lockhart and Martinelli [8] proposed the separated flow model and calculated correlations for two-phase flow resistance. Chisholm [9] concluded the two-phase multiplier as a functional relation to the Martinelli parameter *X*. Scholars revised the *C* value in the Chisholm correlation based on experimental data for various channels. Mishima [10] conducted air-water two-phase flow experiments in small tubes and revised the *C* value as a function of the tube diameter. Sun [11] collected a mass of data for the two-phase flow resistance in mini-channels, proposing a new formation of the Chisholm correlation. They found the *C* value closely related to the ratio of liquid-only and gas-only Reynolds number. Additionally, the exponentiation of the Martinelli parameter was considered a new value rather than one. For two-phase flow resistance in rod bundle channels, the experimental research is limited and the data are deficient. Grant [12] investigated the two-phase pressure drop in a rod bundle arranged in a triangular array with a *Pi/D* of 1.25 and proposed corresponding calculation models. Two-phase flow patterns and frictional pressure drops were experimentally studied by Narrow [13]. The frictional pressure drop was found closely dependent on the flow patterns and the pressure drop cannot be accurately predicted by the homogeneous flow models except for the conditions where the liquid superficial velocities were low enough. Tamai [14] conducted two-phase flow experiments in tight-lattice rod bundle channels with different gap widths and found larger frictional loss in the rod bundles with smaller gap widths. The measured pressure drops were compared with the Martinelli-Nelson's correlation [15] and the results showed that the two-phase frictional pressure drops accounted for a major component. Yan [16] performed

air–water two-phase flow experiments in a 3 × 3 rod bundle under static and rolling motion conditions. They found that the gas flow regime significantly affected the distribution parameter and divided the experimental data into different flow regimes by the gas Reynolds number. A new calculation method for the two-phase frictional pressure drops was proposed based on the Chisholm correlation.

Plenty of studies on flow resistance in various channels. However, few researches on the frictional resistance under natural circulation conditions in rod bundle channels were found in the open literature. In order to explore the flow resistance characteristics under natural circulation conditions, a series of experiments were performed in a 3 × 3 rod bundle channel. The pressure drop results under natural circulation conditions were obtained and the effects of experimental parameters on the frictional resistance were analyzed. Based on the newly obtained experimental results, new correlations were fitted for single-phase and two-phase natural circulation flow in the 3 × 3 rod bundle channel.

2 Experimentation

2.1 Experimental facility

As shown in Fig. 1, the primary circulation loop consists of rod bundle test section, condenser, circulation pump, pressurizer, preheater, filter, electromagnetic flowmeter, valves and pipes. The secondary loop mainly includes cooling tower, water tank and pump, providing the final heat sink for the condenser.

The test section consists of 3 × 3 rod bundle and ceramic partition. Nine hollow heating rods are arranged in square array and the value of *Pi/D* is 1.38, according to the common *Pi/D* range in fuel assemblies and the processing condition. Two grid spacers are respectively fixed near the inlet and the outlet. The rods are connected with a copper plate in the top and a copper column in the bottom and heated by a low-voltage DC power. The max heating power is 45 kW. Outside the channel there is an isolation chamber and the barrel is covered by the insulating layer. Details of test section are shown in Fig. 2.
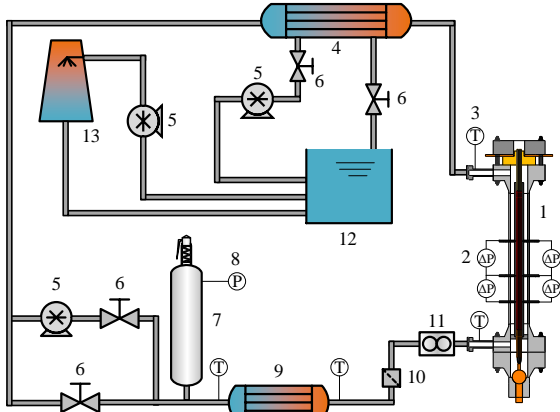
ZHU Zhiqiang, TIAN Chunping, REN Tingting, YAN Changqi, and WANG Jianjun

Fig.1. Experimental loop.

1 test section, 2 differential pressure transmitter,
3 thermocouple, 4 condenser, 5 pump, 6 valve,7 pressurizer,
8 pressure transmitter, 9 preheater,10 filter, 11 electromagnetic
flowmeter, 12 water tank, 13 cooling tower

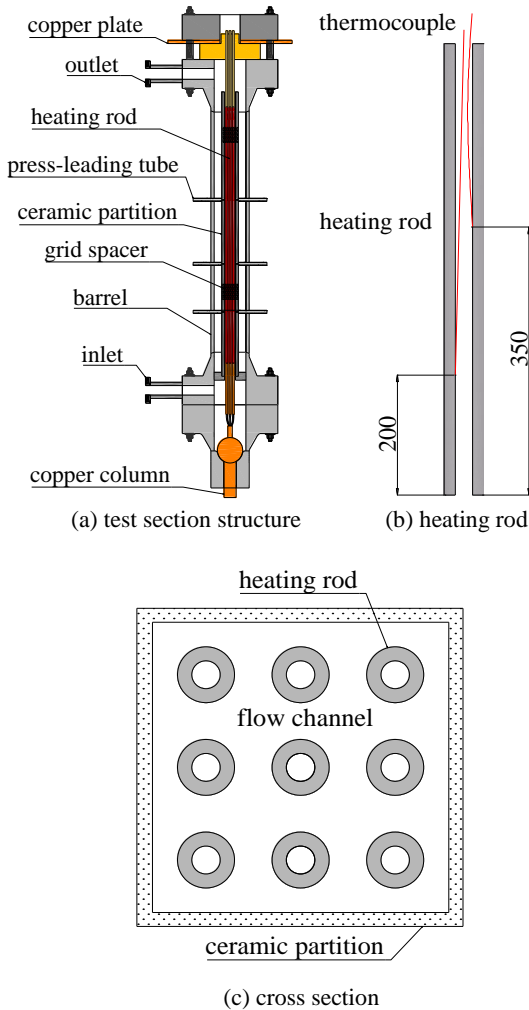(a) test section structure   (b) heating rod

(c) cross section

Fig.2. Rod bundle test section.

Two N-type thermocouples are located at different axial positions inside each heating rod to measure the heating wall temperature along the flow direction.

There are eighteen thermocouples fixed at six different cross sections. The inlet and outlet fluid temperature are measured by two T-type thermocouples and the accuracy of the two kinds of thermocouples are ±0.5 K. There are two pressure measurement sections along the flow direction. The section A contains a grid spacer and the section B does not. The pressure drop in two sections are respectively measured by a Yokogawa EJA110E type and a Rosemount 3051CD type differential pressure transducer, of which the ranges are -1-4 kPa and -1-3 kPa with accuracy of ±0.065% and ±0.05%. The flowrate is measured by KROHNE OPTIFLUX4300 electromagnetic flowmeter. The range and accuracy are respectively -0.5-1 m^3 h^{-1} and ±0.3%.

2.2 Data reduction

For pressure drop processing, the total pressure drop ΔP_t includes gravity pressure drop ΔP_g, frictional pressure drop ΔP_f, acceleration pressure drop ΔP_a and local pressure drop of the grid spacer ΔP_{sg}. ΔP_m is measured value of the differential pressure transducer. The frictional pressure drop is given by the pressure measurement section B. De is hydraulic equivalent diameter of flow channel and G is mass flow rate of the test section. K_{sg} is the local resistance coefficient of the grid spacer and λ is the friction factor.

$$\Delta P_t = \Delta P_g + \Delta P_f + \Delta P_a + \Delta P_{sg} \quad (1)$$

$$\Delta P_t = \Delta P_m + \rho_{tu} gL \quad (2)$$

$$\Delta P_g = \rho_{fl} gL \quad (3)$$

$$\Delta P_a = G^2 \left(\frac{1}{\rho_h} - \frac{1}{\rho_l} \right) \quad (4)$$

$$K_{sg} = \frac{2\rho_{fl}\Delta P_{sg}}{G^2} \quad (5)$$

$$\lambda = \frac{2De\Delta P_f \rho_{fl}}{G^2 L} \quad (6)$$

For a two-phase section, the gravity pressure drop and the acceleration pressure drop are calculated by the separated flow models.

$$\Delta P_{g, tp} = \int_0^{L_{tp}} \left[\rho_l (1-\alpha) + \rho_v \alpha \right] g dl \quad (7)$$

$$\Delta P_{acc, tp} = \int_0^{L_{tp}} \frac{d}{dz} \left\{ G^2 \left[\frac{(1-x)^2}{\rho_l (1-\alpha)} + \frac{x^2}{\rho_v \alpha} \right] \right\} dl \quad (8)$$

where L_{tp} is the two-phase section length and ρ_v denotes the vapor density.

In order to reduce the heat loss, the whole barrel of the test section is covered with two-tier insulating layers and the flow channel is separated with the barrel through an isolation chamber full of stagnant water. The thermal efficiency η for the heating section is calculated by the ratio of the enthalpy increment to the electric power. It is close to unity and never lower than 95% for the stable single-phase flow in all recorded cases. For the two-phase flow, the enthalpy increment is hard to obtain directly. Therefore, the thermal efficiency for the two-phase flow is replaced by the corresponding single-phase thermal efficiency before ONB.

$$\eta = \frac{M \left(h_{out} - h_{in} \right)}{UI} \tag{9}$$

Mass quality is a significant parameter for two-phase pressure drop calculation. Many methods were proposed [17-18], while giving a relatively poor prediction of the mass quality for a low mass flow rate subcooled boiling flow. Sun [19] proposed a model based on thermal equilibrium equations for the Onset of Nucleate Boiling (ONB) and Onset of Saturated Boiling (OSB). Xi [20] found that the model was not completely applicable to the two-phase natural circulation and modified a calculation coefficient based on the natural circulation experimental data. The mass quality in this paper is calculated by the Xi model. The mass quality is calculated as

$$x_{tr} = \begin{cases} 0, \quad x_{eq} < x_{eq,B}; \\ \dfrac{1}{2}\left(x_{eq} - x_{eq,B}\right)\left[\dfrac{\pi^2 \cdot \theta^{2k}}{(2k+1)\cdot 2!} - \dfrac{\pi^4 \cdot \theta^{4k}}{(4k+1)\cdot 4!} + ...\right], \\ \qquad x_{eq,B} \le x_{eq} \le x_{eq,OSB}; \\ x_{eq}, \quad x_{eq,OSB} < x_{eq} < 1 \end{cases} \tag{10}$$

$$x_{eq,B} = \max(x_{eq,in}, x_{eq,ONB}) \tag{11}$$

$$\theta = (x_{eq} - x_{eq,B}) / (x_{eq,OSB} - x_{eq,B}) \tag{12}$$

$$k = 0.032(\rho_l u_{gj} D_{th} / \mu_l)^{0.33}\left[\min\left(1, \frac{x_{eq,in}}{x_{eq,ONB}}\right)\right]^{1.26} \tag{13}$$

$$x_{eq,OSB} = \frac{\left[-\dfrac{\pi^2}{(2k+1)\cdot 2!} + \dfrac{\pi^4}{(4k+1)\cdot 4!} + ...\right]}{\left[2 - \dfrac{\pi^2}{(2k+1)\cdot 2!} + \dfrac{\pi^4}{(4k+1)\cdot 4!} + ...\right]} x_{eq,B} \tag{14}$$

where x_{eq} is the thermodynamic quality and D_{th} is the thermal equivalent diameter.

In the original Xi model, the ONB thermodynamic quality $x_{eq,ONB}$, which is a significant parameter in this model, is calculated by the Miropolskii [21] correlations. However, the predicted locations of ONB are quite different from the experimental values. Therefore, the Jens and Lottes [22] correlation is used to calculate the $x_{eq,ONB}$. The calculated true mass quality and corresponding thermodynamic quality results along the flow direction are shown in Fig. 3. The mass quality of the OSB point is given. The true mass quality value is always greater than 0 and clearly larger than the thermodynamic quality before saturated boiling. With the mass quality increasing, the two kinds of quality are gradually approaching, especially after the OSB point. In this paper, the two-phase flow in the pressure drop measurement section remains in sub-cooled boiling for most experimental conditions. Therefore, the thermodynamic quality and the $x_{eq,ONB}$ are not suitable for the pressure drop calculation. The true mass quality is necessary for the calculation of two phase pressure drop in subcooling region.
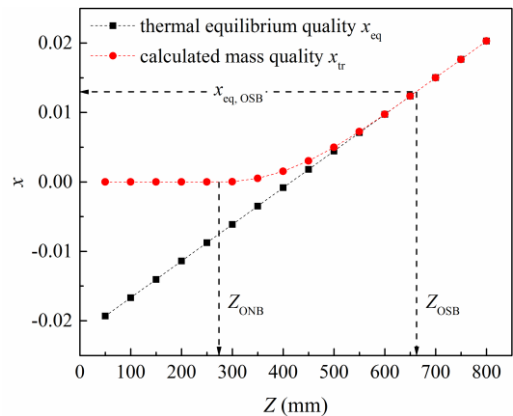

Fig. 3. Calculated mass quality results.

$$\Delta T_{sat,ONB} = 25(q / 10^6)^{0.25} \exp(-P / 6.2) \tag{15}$$

$$x_{eq,ONB} = \frac{h_{ONB} - h_{in}}{h_{fg}} \tag{16}$$

With regard to the void fraction calculation, Chexal [23] developed a method based on the drift flow model for a wide range of two-phase flow conditions and fuel assembly geometries. The void fraction in this paper is calculated by the Chexal–Lellouche correlations, which is used to predict the void fraction in rod bundle channels in the RELAP5/MOD3.2.2 code.

$$C_0 = \frac{L}{K_0 + (1 - K_0)\alpha^r} \tag{17}$$

$$u_{gj} = 1.41\left[\frac{(\rho_1 - \rho_v)\sigma g}{\rho_1^2}\right]^{0.25} C_2 C_3 C_4 C_9 \tag{18}$$

$$\alpha = \frac{j_g}{C_0 j + u_{gj}} \tag{19}$$

where the parameters L, K_0, r and different C values are other parameters in the Chexal–Lellouche correlations. The thermodynamic parameter ranges in the experiments are listed in Table 1.

Table 1 Experimental parameters

Parameters	Range
operating pressure (MPa)	0.1–1.0
heat flux in test section (kW/m²)	5–330
inlet fluid subcooling (K)	10–50
mass flow rate (kg m⁻² s⁻¹)	100–600

2.3 Uncertainty analysis

The N-type and T-type sheathed thermocouples respectively have accuracies of ±1 K and ±0.5 K. The uncertainty for the differential pressure transmitter is ±0.055% and the flow rate has an accuracy of ±0.3%. The heating power is measured with an uncertainty of ±0.5%. Kline & McClintock [24] methodology is used to calculate and evaluate the uncertainties of computed results. For the experimental parameters in this paper, the calculated relative uncertainty ranges for friction factors and local resistance coefficients are respectively 3.2–10.5% and 2.8–6.1%. The relative uncertainty ranges for mass quality and void fraction are respectively 6.2–10.4% and 7.1–11.3%. Moreover, the relative uncertainty range for the two-phase frictional pressure drop is 8.5–14.0%.

3 Results and discussions

3.1 Single-phase flow resistance characteristics

Under system pressure 0.3 MPa and heating power 3kW, groups of natural circulation experiments with the inlet subcooling degree 30-90 K were conducted to obtain the flow resistance results, shown in Fig. 4.

With regard to the friction factor in rod bundle channel, there is no theoretical solution at present, so the friction factor prediction is mainly based on experimental results. Cheng & Todreas analyzed a large amount of experimental data and proposed friction factor prediction correlations for different flow regimes. The laminar and turbulent friction factor are respectively expressed as

$$\lambda_L = C_L / Re \tag{20}$$

$$\lambda_T = C_T / Re^{0.18} \tag{21}$$

$$\lambda_{tr} = \lambda_L (1 - \varphi)^{1/3} + \lambda_T \varphi^{1/3} \tag{22}$$

$$\varphi = \frac{\log(Re) - \log(Re_L)}{\log(Re_T) - \log(Re_L)} \tag{23}$$

C_L and C_T can be obtained by Cheng & Todreas [3]. Re_L and Re_T are calculated by the value of Pi/D.
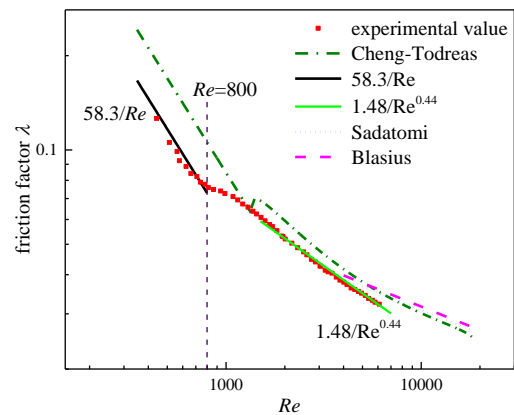

Fig.4. Friction factor in natural circulation condition.

As shown in Fig. 4, the friction factor experimental values are generally lower than Cheng & Todreas correlations especially in low Reynolds number region. It is observed that the friction factor slope changes obviously near Reynolds number 800 and the transition Reynolds number is considered to be 800, which is reasonable according to the common range of the transition Reynolds number. Owing to the specific channel structure, the transverse disturbance is easy to occur, so the transition

Reynolds number in rod bundle channel is rather different from the regular channel. The trend of experimental results and Cheng & Todreas results is consistent while the experimental friction factors are lower than those of Cheng & Todreas. First, Cheng & Todreas correlation is fitted by the experimental results for a 37-pin wire-wrapped rod bundle. The wire-wrapped structure makes the friction factor results larger than those for bare rod bundles in the same Reynolds number. Second, experiments in this paper are performed under natural circulation conditions while Cheng & Todreas results are from isothermal and adiabatic experiments. Therefore, the fluid viscosity near the heating surface in this study is lower than that of the bulk flow because of the temperature gradient, even though Reynolds number covers the viscosity effect at bulk temperature. Moreover, higher fluid viscosity near the heating surface makes the flow resistance lower than isothermal and adiabatic results, which accounts for the differences between Cheng & Todreas and the experimental results. In laminar regime, the friction factor and the Reynolds number basically meet the formation of Eq. (20). Based on the experimental results, friction factor prediction correlation for laminar flow is fitted as

$$\lambda=58.3 / Re \qquad (24)$$

The Reynolds number range is 300-800 and the relative error of fitted correlation and the experimental values is within 5%. In addition, there is no obvious change of friction factor until the Reynolds number reaches 7000, which indicates that in rod bundle channel the transition regime under natural circulation condition is still wide. It is accordant with the conclusion of Cheng & Todreas [3], namely, the wall and rod shear stress makes the flow regime transition hard to occur and it develops from the channel center to the wall surface. In the Reynolds number range 1500-7000, another correlation is fitted to predict the friction factor in transition regime and the relative error is within 5%.

$$\lambda=1.48Re^{-0.44} \qquad (25)$$

Different from regular channel, the grid spacer is necessary for rod bundle channel to fix the rods and also an important local restrictive device. Since there are various grid spacer types, the local resistance coefficient is hard to express by a single correlation.

The local resistance coefficient of grid spacer is mainly obtained from experiments. Figure 5 shows the grid spacer local resistance coefficient results under the working condition that is the same as Fig. 4.
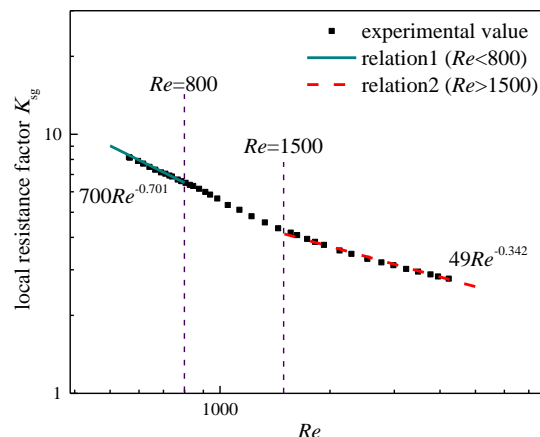

Fig. 5. Local resistance coefficient in natural circulation condition.

It is clear in Fig. 5 that the slope of local resistance coefficient has slight change near Reynolds number 800. Similarly, two correlations for grid spacer local resistance coefficient prediction are fitted when *Re*<800 and *Re*>1500. The relative error of fitted correlations and the experimental values are both within 5%.

$$K_{sg1}=700Re^{-0.701} \qquad (26)$$

$$K_{sg2}=49Re^{-0.342} \qquad (27)$$

3.2 Two-phase flow resistance characteristics

In this section, the boiling flow phases are identified. The ONB during the experiment is determined by the wall temperature drop. The variation of pressure drop components, including the gravity pressure drop, the frictional pressure drop and the acceleration pressure drop, is given. For high mass quality conditions, the mass flow rate is observed declining with the increasing heat flux.

3.2.1 Determination of two-phase section

Different from air-water two-phase flow, the boiling flow resistance is much more complex. Since the boiling flow is developing along the flow channel, the determination of the two-phase section is important. Additionally, the flow instability, which is undesirable in the experiments, may occur with the increasing heat flux. In order to accurately investigate

the boiling flow resistance, a stable two-phase flow needs to be obtained. Figure 6 shows the flow rate and pressure drop changes with the increasing heat flux in single-phase, two-phase and instability regions. For the subcooled boiling flow, the flow instability occurs when the heat flux increases at the t_b moment. For the saturated boiling flow, methods such as decreasing inlet fluid subcooling degree and increasing local resistance at the inlet are adopted to restrain the flow instability. Thus obtaining the stable saturated boiling flow at the t_c moment with the increasing heat flux. In this paper, the flow resistance in the two-phase regions are focused.

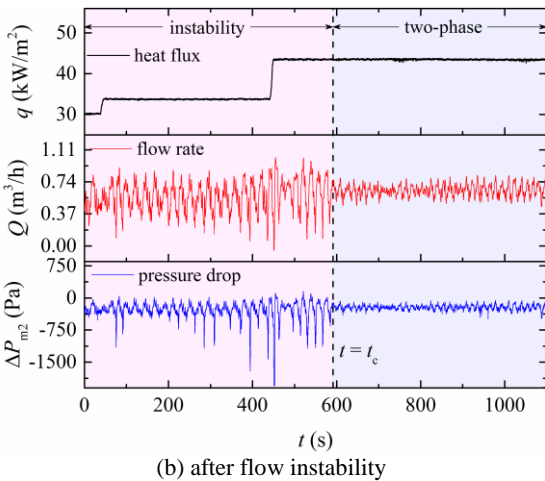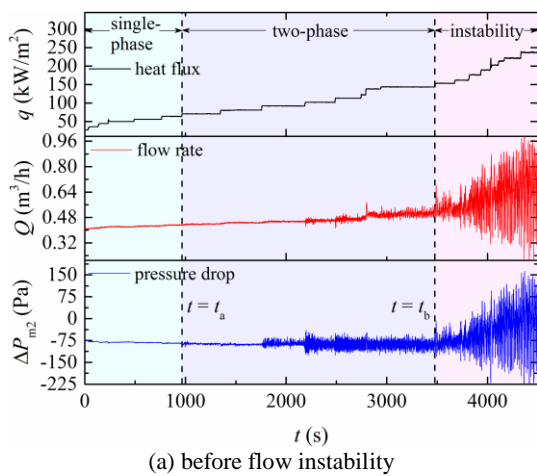(a) before flow instability

(b) after flow instability

Fig. 6. Different phases in flow boiling.

Apart from the flow phases, the two-phase section length is significant as well. As the demarcation point between the single-phase and the two-phase regions, ONB locations significantly affect the two-phase frictional pressure drops calculation. The ONB in this study is identified by the abrupt decrease of wall temperature. Limited by the measuring points distribution and based on experimental ONB

locations, the Jens and Lottes correlations are used to calculate the $x_{eq, ONB}$. In order to verify the accuracy of the calculated ONB locations, Fig. 7 shows the calculated ONB location results and corresponding experimental ONB regions with different heat fluxes. It is clear that the variation tendency of the calculated values is reasonable and consistent with the experimental regions. The majority of the calculated locations are within the experimental ONB regions. The Jens and Lottes correlation is considered applicable for the ONB location prediction in the experiments, especially when the ONB location is near the outlet of the heating section, namely for relatively lower heat flux.
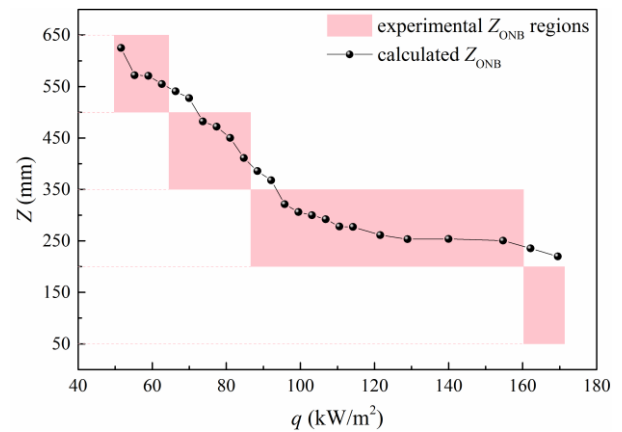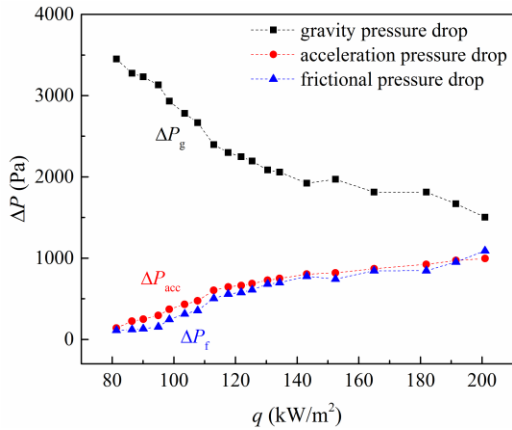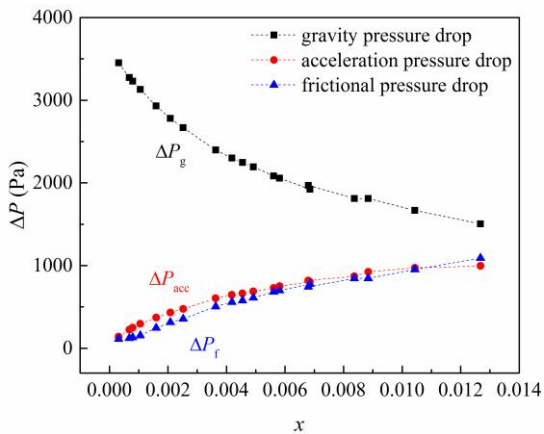

Fig. 7. ONB location variation with heat flux.

3.2.2 Two-phase pressure drop variation

The two-phase pressure drops are composed of the gravity pressure drop, the frictional pressure drop and the acceleration pressure drop. Figure 8 shows the pressure drops variation with the heat flux and mass quality. With the heat flux increasing, the gravity pressure drop decreases but the frictional pressure drop and the acceleration pressure drop increases. The pressure drops change rapidly first and then the variation tends to be gentle because the void fraction varies fast in the low mass quality conditions. When the saturated boiling is full of the whole pressure drop measurement section, the pressure drop becomes insensitive to the mass quality as well as the heat flux. Additionally, the acceleration pressure drop increases faster and is larger than the frictional pressure drop in the low mass quality conditions. However, in the high mass quality conditions, the frictional pressure drop increases a little faster than the acceleration pressure drop.

(a) pressure drops variation with heat flux

(b) pressure drops variation with mass quality
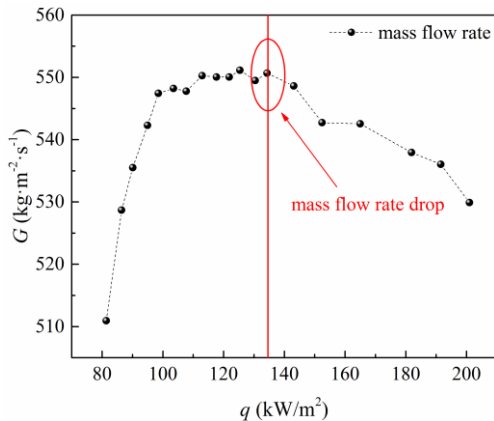
Fig. 8. Pressure drops variation.

Fig. 9. Mass flow rate variation with heat flux.

Figure 9 shows the mass flow rate variation with the heat flux. The mass flow rate first increases in the low mass quality conditions and then stay approximately unchanged. When the heat flux continues increasing, the mass flow rate decreases with the heat flux, which means that the resistance grows faster than the gravity pressure drop reduction. It is different from the forced circulation.

3.3 New correlation for two-phase frictional pressure drop

Chisholm [9] proposed a correlation for the two-phase multiplier based on the Martinelli parameter X. The parameter C is significant and many researchers revised it based on different experimental data. In view of the poor prediction for the experimental pressure drop by the Chisholm correlation, a new correlation form is proposed as the Eq. (28).

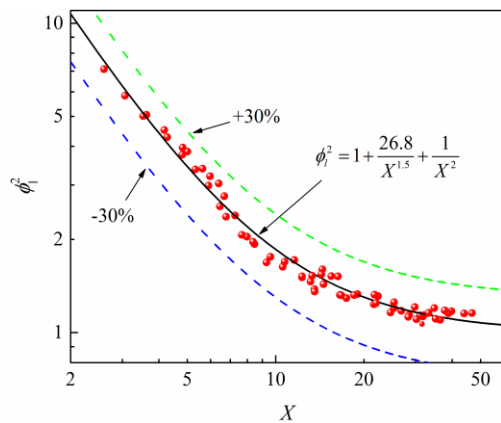$$\phi_l^2 = 1 + \frac{C}{X^n} + \frac{1}{X^2} \quad (28)$$

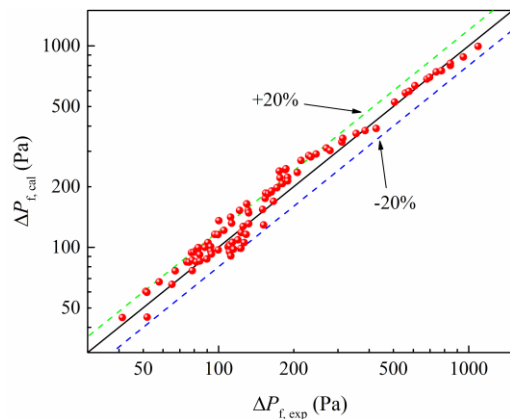Fig. 10. Comparison of new correlation results.

Fig. 11. Comparison of experimental data.

The fitted correlation is shown in Fig. 10 and the parameter C and the power n are respectively 26.8 and 1.5. Figure 11 shows the comparison of experimental data and predicted two-phase frictional pressure drops by the new correlation. The relative errors of more than 90% predicted values are within ±20% and the overall mean relative error is 12.5%.

According to the comparison with the experimental data, the relative errors are within acceptable limits. Thus the calculation results of the fitted correlation are reasonable and valid. The new correlation is

considered applicable for the two-phase frictional pressure drops prediction in the rod bundle channel under natural circulation conditions. The applicative flow condition ranges included the system pressure 0.1–1 MPa, the mass flow rate 100–600 kg m^{-2} s^{-1} and the mass quality 0–0.13.

4 Conclusions

Flow resistance characteristics under natural circulation conditions in a 3 × 3 rod bundle channel are experimentally studied in this paper. The frictional resistance and the grid spacer local resistance were analyzed. The flow boiling phases are identified and boiling pressure drops components variation is studied. New correlations are fitted based on the experimental results for both single- phase and two-phase flow.

1) The flow regime is divided and the transition Reynolds number is about 800. The friction factor results are generally smaller than the Cheng & Todreas correlation. Based on the experimental results, friction factor prediction correlations for laminar and transition flow are fitted and the relative error is less than 5%. In addition, another two correlations are fitted for the prediction of grid spacer local resistance coefficient in different Reynolds number ranges.

2) With the increasing heat flux, the flow instability occurs easily under natural circulation subcooled boiling conditions. The flow phases recognition for the stable flow is necessary. The wall temperature drop method for the ONB determination is applicable for the experiments.

3) The gravity pressure drops decrease while the frictional pressure drops and the acceleration pressure drops increase with the increasing heat flux. The acceleration pressure drops increase faster than the frictional pressure drops under the low mass quality conditions. For high mass quality conditions, if the resistance including frictional pressure drop and the acceleration pressure drop grows even faster than the gravity pressure drop reduction, the mass flow rate decreases with the increasing heat flux.

4) In the form of the Chisholm correlation, a new correlation for the two-phase frictional pressure drop is fitted by the experimental results. The new correlation is compared with the experimental results for the reasonability and validity. Under the given flow conditions, the new correlation can well predict the two-phase frictional pressure drops in the experiments with a mean relative error of 12.5%.

Nomenclature

D	rod outer diameter, m
De	hydraulic equivalent diameter, m
D_{th}	thermal equivalent diameter, m
g	gravity acceleration, m/s^2
G	mass flow rate, kg/(m^2 s)
h	enthalpy, kJ/kg
h_{fg}	latent heat of vaporization, kJ/kg
K	local resistance coefficient
L	pressure measurement section length, m
Pi	rod pitch, m
q	heat flux, kW/m^2
Re	Reynolds number
T	temperature, K
x	mass quality
ΔP_a	acceleration pressure drop, Pa
ΔP_f	frictional pressure drop, Pa
ΔP_g	gravity pressure drop, Pa
ΔP_m	measured pressure drop, Pa
ΔP_{sg}	local pressure drop, Pa
ΔP_t	total pressure drop, Pa
α	void fraction
β	volume void fraction
μ	dynamic viscosity, Pa s
σ	surface tension, N/m
λ	friction factor
ρ	density, kg/m^3
φ	intermittency factor

Subscripts

B	Boiling
cal	calculation
eq	equilibrium
exp	experimental
fl	fluid
in	inlet
l	liquid
L	Laminar
sat	saturation
sg	grid spacer
sp	single-phase
tp	two-phase
tr	true
tu	tube
T	Turbulent
v	vapor

Acknowledgments

References

[1] REHME, D.I.K, *et al.*: Laminarströmung in Stabbündeln [J]. Chemie Ingenieur Technik, 1971, 43(17): 962-966.

[2] REHME, K., *et al.*: Simple method of predicting friction factors of turbulent flow in non-circular channels [J]. International Journal of Heat & Mass Transfer, 1973, 16(5): 933-950.

[3] CHENG, S K., and TODREAS, N.E, *et al.*: Hydrodynamic models and correlations for bare and wire-wrapped hexagonal rod bundles — bundle friction factors, subchannel friction factors and mixing parameters [J]. Nuclear Engineering & Design, 1986, 92(2): 227-251.

[4] YAN, C., CAO, X., and YAN, C., *et al.*: Effects of rolling on resistance characteristics of single-phase flow in a 3×3 rod bundle [J]. Progress in Nuclear Energy, 2015, 78: 231-239.

[5] MAREK, M.J.: Heat transfer and pressure drop performance of rod bundles arranged in square arrays, International Journal of Heat and Mass Transfer, 16(1973) 2215-2228.

[6] LEE, K.: Analytical prediction of subchannel friction factor for infinite bare rod square and triangular arrays of low pitch to diameter ratio in turbulent flow, Nuclear Engineering & Design, 157(1995) 197-203.

[7] EIFLER, W.R.: Nijsing, Experimental investigation of velocity distribution and flow resistance in a triangular array of parallel rods, Nuclear Engineering & Design, 5(1967) 22-42.

[8] W. L R.: Proposed Correlation of Data for Isothermal Two-Phase, Two-Component Flow in Pipes [J]. Chem.eng.prog, 1949, 4539-48. 1949.

[9] CHISHOLM, D.: A theoretical basis for the Lockhart-Martinelli correlation for two-phase flow [J]. International Journal of Heat & Mass Transfer. 1967, 10(12): 1767-1778.JIANG, M. H., XU, H. J., & DAI, Z. M.: Advanced fission energy program-TMSR nuclear energy system, Bulletin of Chinese Academy of Sciences, 2012, 27(3):366-374.

[10] MISHIMA, K., and HIBIKI, T.: Some characteristics of air-water two-phase flow in small diameter vertical tubes [J]. International Journal of Multiphase Flow. 1996, 22(4): 703-712.

[11] SUN, L, and MISHIMA, K.: Evaluation analysis of prediction methods for two-phase flow pressure drop in mini-channels [J]. International Journal of Multiphase Flow. 2009, 35(1): 47-54.

[12] GRANT, I.D.R.: Murray I. Pressure drop on the shell-side of a segmentally baffled shell-and-tube heat exchanger with vertical two-phase flow [M]. National Engineering Laboratory, 1972.

[13] NARROW, T.L., GHIAASIAAN, S.M., and ABDEL-KHALIK, S.I., *et al.*: Gas–liquid two-phase flow patterns and pressure drop in a horizontal micro-rod bundle [J]. International Journal of Multiphase Flow. 2000, 26(8): 1281-1294.

[14] TAMAI, H., KURETA, M., and OHNUKI, A., *et al.*: Pressure Drop Experiments using Tight-Lattice 37-Rod Bundles [J]. Journal of Nuclear Science & Technology. 2006, 43(6): 699-706.

[15] R.C. MARTINELLI, D B N.: Prediction of pressure drop during forced-circulation boiling of water [J]. Trans. 1948, 70: 695-702.

[16] YAN, C., SHEN, J., and YAN, C., *et al.*: Resistance characteristics of air–water two-phase flow in a rolling 3×3 rod bundle [J]. Experimental Thermal and Fluid Science. 2015, 64: 175-185.

[17] S.L.: Forced convection subcooled boiling—prediction of vapor volumetric fraction [J]. International Journal of Heat & Mass Transfer, 1967, 10(7)951-965. [J]. 1967.

[18] SAHA, P., and ZUBER, N.: Point of net vapor generation and vapor void fraction in subcooled boiling [J]. Analyst. 1974, 112(3): 259-261.

[19] SUN, Q., YANG, R., and TAN, S., *et al.*: Prediction of true mass quality in subcooled steam-water flow boiling [J]. Journal of Tsinghua University. 2004, 44(11): 1580-1584.

[20] XI, Z., SUN, Q., and CHEN, J., *et al.*: Predictive and Experimental Study of Cross-Section Average Void Fraction in Sub-Cooled Boiling with Natural Circulation [J]. Nuclear Power Engineering. 2005(04): 312-316.

[21] MIROPOLSKII Z.L.S.P.E.A.: Void Fraction of water-steam mixture flow with or without heat transfer [J]. Teploenergetika. 1971, 5: 374-379.

[22] JENS, W.H.L.P.A.: Analysis of Heat Transfer, Burnout, Pressure Drop and Density Data for High Pressure Water [J]. Boiling. 1951, 2(9): 51-59.

[23] CHEXAL, B.H.J.L.A.: Void Fraction Correlation for Generalized Applications [J]. 1986.

[24] MCCLINTOCK, S.K.F.: Describing Uncertainties in Single Sample Experiments [J]. 1953.